THE JOURNAL OF PHYSICAL CHEMISTRY B

Article

pubs.acs.org/JPCB

Estimating Side-Chain Order in [U-^{2}H;^{13}CH$_3$]-Labeled High Molecular Weight Proteins from Analysis of HMQC/HSQC Spectra

Vitali Tugarinov*,† and Lewis E. Kay‡

†Department of Chemistry and Biochemistry, University of Maryland, College Park, Maryland 20742, United States

‡Departments of Molecular Genetics, Biochemistry, and Chemistry, University of Toronto, Toronto, Ontario, Canada M5S 1A8, and Program in Molecular Structure and Function, Hospital for Sick Children, 555 University Avenue, Toronto, Ontario, Canada M5G 1X8

Supporting Information

ABSTRACT: A simple approach for quantification of methyl-containing side-chain mobility in high molecular weight methyl-protonated, uniformly deuterated proteins is described, based on the measurement of peak intensities in methyl ^{1}H−^{13}C HMQC and HSQC correlation maps and relaxation rates of slowly decaying components of methyl ^{1}H−^{13}C multiple-quantum coherences. A strength of the method is that [U-^{2}H;^{13}CH$_3$]-labeled protein samples are required that are typically available at an early stage of any analysis. The utility of the methodology is demonstrated with applications to three protein systems ranging in molecular weight from 82 to 670 kDa. Although the approach is only semiquantitative, a high correlation between order parameters extracted via this scheme and other more established methods is nevertheless demonstrated.

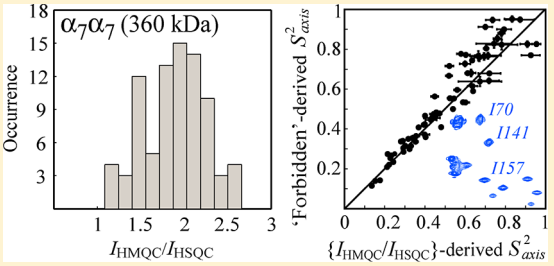

INTRODUCTION

Solution NMR spectroscopy studies of high molecular weight proteins and protein complexes have been greatly expanded by the introduction of labeling schemes that lead to the production of uniformly deuterated, methyl-protonated proteins[1−9] and the subsequent development of experiments that exploit the unique properties of the labels.[8−11] Included in the list of such experiments are those that probe methyl-containing side-chain dynamics.[8] For example, ^{13}CHD$_2$ methyl isotopomers have been used to quantify picosecond−nanosecond time scale motions using either ^{13}C or ^{2}H spins in a variety of high molecular weight proteins and protein complexes.[12−18] Other, related experiments take advantage of ^{1}H−^{1}H dipolar cross-correlation spin relaxation networks in ^{13}CH$_3$ methyl groups to extract similar information.[8,19−21] Each of these different types of experiment has advantages and disadvantages, but all share the problem of sensitivity as the aggregate molecular weights of the systems investigated increase.

Studies involving the ^{13}CH$_3$ "class" of methyl groups are appealing because [U-^{2}H;^{13}CH$_3$]-labeled proteins are typically produced during the initial stages of a project and are therefore available for analysis from the outset. With this in mind, we have previously developed a "^{13}CH$_3$-based" experiment that exploits a methyl-TROSY (transverse relaxation-optimized spectroscopy) effect[10,22] for the measurement of millisecond time scale dynamics in high molecular weight proteins,[23] as well as companion experiments for the studies of picosecond−nanosecond motions.[20,21] The latter experiments rely on the buildup of methyl ^{1}H double-quantum (2Q) or triple-quantum (3Q) coherences, providing a sensitive measure of differential ^{1}H relaxation within the methyl spin system that, for practical applications, can only be exploited when the overall molecular tumbling is slow. While these relaxation-violated coherence transfer based experiments have been successfully applied in the studies of a single ring of the proteasome (180 kDa) and of the 360 kDa 1/2-proteasome,[8,9,20,21] our goal is to develop additional experiments that provide increased sensitivity so that applications can extend to even higher molecular weight systems.

Because the simplest of pulse schemes often tend to be those that produce spectra of the highest sensitivity, we asked whether data sets generated from HMQC[24,25] and HSQC[26] experiments recorded on [U-^{2}H;^{13}CH$_3$]-labeled proteins might be used to provide at least a qualitative measure of fast time scale dynamics. Intuitively, this seems likely. For example, enhancements obtained in TROSY-based spectra involving amide ^{1}H−^{15}N,[27] aromatic ^{1}H−^{13}C,[28] "static" methylene ^{13}CH$_2$,[29] or fast-rotating ^{13}CH$_2$(D)[14] spin systems depend on local dynamics at the site of interest. In a similar manner, we have previously shown that relative intensities of methyl correlations measured using the HMQC experiment, which exploits a methyl-TROSY effect, versus HSQC, which does not, are also a function of dynamics.[10] Here, we describe a simple approach for the semiquantitative evaluation of side-chain mobility in high molecular weight [U-^{2}H;^{13}CH$_3$]-labeled proteins based on an analysis of experimental peak intensities

Received: January 30, 2013
Revised: March 3, 2013
Published: March 4, 2013

   dx.doi.org/10.1021/jp401088c | J. Phys. Chem. B 2013, 117, 3571−3577

in HMQC (I_{HMQC}) and HSQC (I_{HSQC}) data sets supplemented by relaxation rates of the slowly decaying component of the methyl $^1H-^{13}C$ MQ coherence, R^S_{MQ}. Methyl order parameters squared, S_{axis}^2, obtained from I_{HMQC}/I_{HSQC} ratios, are compared with those derived from the 3Q-"forbidden" relaxation-violated coherence transfer scheme that has recently been validated.[21] The approach is demonstrated with several protein systems, including [U-^{2}H;Ile$^{\delta1}$-^{13}CH$_3$]-malate synthase G (MSG, 82 kDa),[11,30] [U-^{2}H;Ile$^{\delta1}$-^{13}CH$_3$;Leu,Val-^{13}CH$_3$/^{12}CD$_3$]-$\alpha_7\alpha_7$ (1/2-proteasome, 360 kDa),[17] and the [U-^{2}H;Ile$^{\delta1}$-^{13}CH$_3$;Leu,Val-^{13}CH$_3$/^{12}CD$_3$]-labeled 20S proteasome core particle (20S CP, $\alpha_7\beta_7\beta_7\alpha_7$, 670 kDa)[17,31] with ILV methyl labeling restricted to the two α_7 heptameric rings.

MATERIALS AND METHODS

Protein Samples. All protein samples were prepared as described previously[10,17,32] using [U-^{2}H]glucose as the main carbon source and appropriate α-keto acid precursors for selective methyl labeling.[4,6] Sample conditions were 0.25 mM MSG, 99.9% D_2O, 25 mM sodium phosphate, pH 7.1, 5 mM $MgCl_2$, 0.05% NaN_3, 5 mM DTT; and 0.14 mM $\alpha_7\alpha_7$ and 0.21 mM $\alpha_7\beta_7\beta_7\alpha_7$ (concentrations of complexes), 99.9% D_2O, 25 mM potassium phosphate, pH 6.8, 50 mM NaCl, 1 mM EDTA, 0.03% NaN_3, and 2 mM DTT.

NMR Spectroscopy and Data Analysis. Experiments on $\alpha_7\alpha_7$ and $\alpha_7\beta_7\beta_7\alpha_7$ were measured on an 800 MHz Varian Inova spectrometer, while NMR measurements on MSG were carried out at 600 MHz using a Bruker Avance III spectrometer, with both instruments equipped with room-temperature triple-resonance probes. Acquisition times $t_{1,max}$ = 100 (50, 30) ms were used for MSG ($\alpha_7\alpha_7$, $\alpha_7\beta_7\beta_7\alpha_7$), while $t_{2,max}$ was 64 ms in all cases. To minimize possible errors in relative peak intensities resulting from different numbers of pulses in HMQC and HSQC sequences and hence differential effects from radio frequency pulse imperfections, HMQC experiments have been implemented with simultaneous ^1H and ^{13}C 180° pulses in the middle of $^1H\rightarrow{}^{13}C$ and $^{13}C\rightarrow{}^1H$ INEPT transfer steps. In this manner, the same number of 180° pulses are applied in both schemes, although an extra pair of ^1H 90° pulses is necessary for recording the HSQC data set. All NMR spectra were processed and analyzed using the NMRPipe/NMRDraw suite of programs and associated software.[33] HMQC and HSQC spectra of MSG and $\alpha_7\alpha_7$ were not apodized in either dimension for extraction of I_{HMQC}/I_{HSQC} ratios. In contrast, apodization of FIDs with cosine-bell functions in both dimensions was used for analysis of $\alpha_7\beta_7\beta_7\alpha_7$ data to maximize the number of correlations that could be quantified (significant differences in I_{HMQC}/I_{HSQC} ratios were not observed for peaks analyzed with and without apodization). Errors in S_{axis}^2 were estimated by a Monte Carlo-type analysis[34] via multiple searches for S_{axis}^2 using (i) experimental uncertainties in I_{HMQC}/I_{HSQC} ratios obtained from duplicate or triplicate measurements and (ii) experimental random errors in R^S_{MQ} rates extracted from a Monte Carlo simulation of single-exponential fits with the spectral noise-floor taken as an estimate of random uncertainties in peak intensities. The average random uncertainties in I_{HMQC}/I_{HSQC} (R^S_{MQ}) are 1.1% (1.5%), 1.5% (2.0%), and 4.1% (6.2%) in MSG, $\alpha_7\alpha_7$, and $\alpha_7\beta_7\beta_7\alpha_7$, respectively.

RESULTS AND DISCUSSION

As a prelude to understanding how the relative peak intensities in HSQC and HMQC data sets can be used to extract information about side-chain order in high molecular weight proteins, it is instructive to consider the expressions for I_{HSQC} and I_{HMQC} as a function of the acquisition times, t_1 and t_2,

$$\begin{aligned} I_{HSQC}(t_1, t_2) = & \\ & [(9/4)\exp(-2\tau R^F_{2,H}) + (9/4)\exp(-2\tau R^S_{2,H})] \\ & \times \exp(-2\tau R^F_{2,H})\exp(-t_1 R^F_{2,C})\exp(-t_2 R^F_{2,H}) \\ & + [(9/4)\exp(-2\tau R^F_{2,H}) - (3/4)\exp(-2\tau R^S_{2,H})] \\ & \times \exp(-2\tau R^F_{2,H})\exp(-t_1 R^S_{2,C})\exp(-t_2 R^F_{2,H}) \\ & + [(9/4)\exp(-2\tau R^F_{2,H}) + (9/4)\exp(-2\tau R^S_{2,H})] \\ & \times \exp(-2\tau R^S_{2,H})\exp(-t_1 R^F_{2,C})\exp(-t_2 R^S_{2,H}) \\ & + [-(3/4)\exp(-2\tau R^F_{2,H}) + (9/4)\exp(-2\tau R^S_{2,H})] \\ & \times \exp(-2\tau R^S_{2,H})\exp(-t_1 R^S_{2,C})\exp(-t_2 R^S_{2,H}) \end{aligned} \quad (1)$$

and

$$\begin{aligned} I_{HMQC}(t_1, t_2) = & \\ & 6\exp(-4\tau R^F_{2,H})\exp(-t_1 R^F_{MQ})\exp(-t_2 R^F_{2,H}) \\ & + 6\exp(-4\tau R^S_{2,H})\exp(-t_1 R^S_{MQ})\exp(-t_2 R^S_{2,H}) \end{aligned} \quad (2)$$

that have been derived previously.[10,22] Here, we have assumed that the molecule tumbles slowly, $\omega_C\tau_C \gg 1$, where ω_C is the ^{13}C resonance frequency and τ_C is the (isotropic) global correlation time, and that methyl rotation is infinitely fast. The superscripts "F" and "S" denote the "fast" and "slow" transverse relaxation rates of ^1H single-quantum (SQ) (subscript "2,H"), ^{13}C SQ ("2,C") or $^1H-^{13}C$ multiple-quantum ("MQ") coherences. The relaxation rates can, in turn, be recast as

$$R^F_{2,H} = \left\{\left(\frac{9}{20}\right)\frac{\gamma_H^4\hbar^2\tau_C}{r_{HH}^6} + \left(\frac{1}{45}\right)\frac{\gamma_H^2\gamma_C^2\hbar^2\tau_C}{r_{HC}^6}\right\}\left(\frac{\mu_0}{4\pi}\right)^2 \times S^2_{axis} + R_{2,ext} \quad (3.1)$$

$$R^S_{2,H} = \left\{\left(\frac{1}{45}\right)\left(\frac{\mu_0}{4\pi}\right)^2\frac{\gamma_H^2\gamma_C^2\hbar^2\tau_C}{r_{HC}^6}\right\}S_{axis}^2 + R_{2,ext} \quad (3.2)$$

$$R^F_{2,C} = \left\{\left(\frac{1}{5}\right)\left(\frac{\mu_0}{4\pi}\right)^2\frac{\gamma_H^2\gamma_C^2\hbar^2\tau_C}{r_{HC}^6}\right\}S_{axis}^2 + R_{1,ext} \quad (3.3)$$

$$R^S_{2,C} = \left\{\left(\frac{1}{45}\right)\left(\frac{\mu_0}{4\pi}\right)^2\frac{\gamma_H^2\gamma_C^2\hbar^2\tau_C}{r_{HC}^6}\right\}S_{axis}^2 + R_{1,ext} \quad (3.4)$$

$$R^F_{MQ} = \left\{\left(\frac{4}{45}\right)\frac{\gamma_H^2\gamma_C^2\hbar^2\tau_C}{r_{HC}^6} + \left(\frac{9}{20}\right)\frac{\gamma_H^4\hbar^2\tau_C}{r_{HH}^6}\right\}\left(\frac{\mu_0}{4\pi}\right)^2 \times S^2_{axis} + R_{2,ext} \quad (3.5)$$

$$R^S_{MQ} = R_{2,ext} \quad (3.6)$$

dx.doi.org/10.1021/jp401088c | J. Phys. Chem. B 2013, 117, 3571−3577

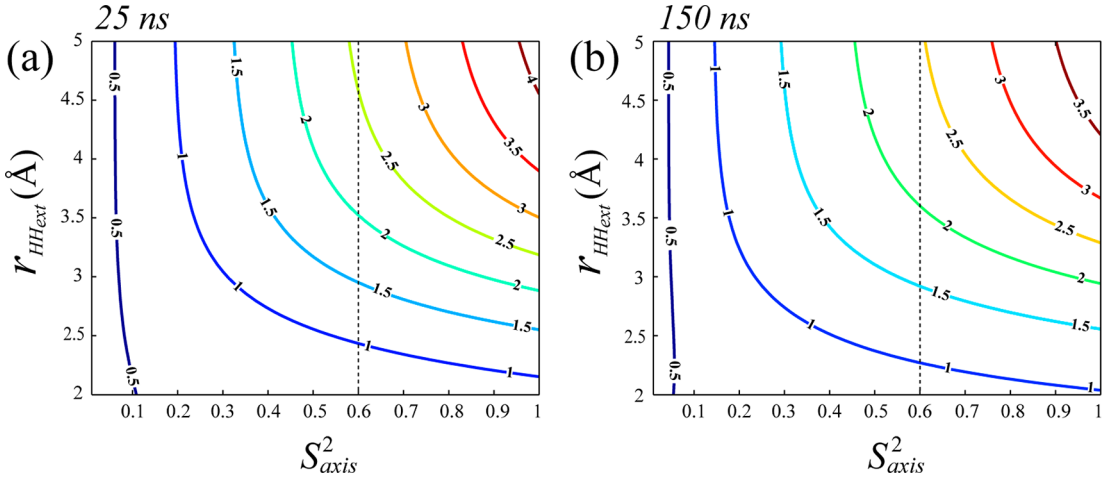

Figure 1. Contour plots of I_{HMQC}/I_{HSQC} ratios calculated as a function of S_{axis}^2 and r_{HHext} (Å) for overall molecular tumbling times τ_C of (a) 25 ns and (b) 150 ns. Acquisition times $t_{2,max}$ = 64 ms and $t_{1,max} = (3/R^S_{MQ})$ ms have been used in all calculations. The value of r_{HDext} has been set to 1.8 Å and τ = 2.0 ms. Dashed vertical lines are drawn at S_{axis}^2 = 0.6, the value at which S_{axis}^2 is fixed in Figure 2.

$$R_{2,ext} = \left(\frac{8}{15}\right)\left(\frac{\mu_0}{4\pi}\right)^2 \frac{\gamma_H^2\gamma_D^2\hbar^2\tau_C}{r_{HDext}^6} + \left(\frac{9}{20}\right)\left(\frac{\mu_0}{4\pi}\right)^2 \frac{\gamma_H^4\hbar^2\tau_C}{r_{HHext}^6} \tag{3.7}$$

$$R_{1,ext} = \left(\frac{3}{20}\right)\left(\frac{\mu_0}{4\pi}\right)^2 \frac{\gamma_H^4\hbar^2\tau_C}{r_{HHext}^6} \tag{3.8}$$

In eqs 3.1−3.8 μ_0 is the vacuum permeability constant, S_{axis} is an order parameter describing the amplitude of motion of the methyl 3-fold axis, γ_j is the gyromagnetic ratio of spin j, r_{HC} (1.135 Å) and r_{HH} (1.813 Å) are distances between H−C and H−H spins within the methyl group, and the defocusing/refocusing time for in-phase/antiphase ^{1}H magnetization in the HSQC/HMQC pulse schemes is 2τ, which is typically set to $\sim(2^1J_{CH})^{-1}$ = 4.0 ms. Dipolar spin relaxation contributions from external protons and deuterons are given by $R_{2,ext}$ and $R_{1,ext}$, with

$$r_{HHext} = \frac{1}{3}\sum_{j=1-3}\left(\sum_i \frac{1}{r_{H_j,H_i}^6}\right)^{-1/6}$$

and

$$r_{HDext} = \frac{1}{3}\sum_{j=1-3}\left(\sum_i \frac{1}{r_{H_j,D_i}^6}\right)^{-1/6}$$

where the inner summation is over all protons or deuterons i in the protein, proton j is attached to the methyl in question ($i \neq j$), and the outer summation averages over the three methyl protons. In eqs 3.7 and 3.8 an order parameter of unity has been assumed.[10] Note that the factor (9/20) in eq 3.7 includes the effects of dipole−dipole cross-correlations between methyl protons and external ^{1}H spins, which were not taken into account in our original work.[22] Relaxation contributions from either ^{1}H or ^{13}C chemical shift anisotropy (CSA) have been neglected in the above equations, although they could easily be included (see below).

Expressions for the maximum intensity of each cross-peak (i.e. on-resonance) in HSQC and HMQC data sets are readily obtained by replacing $\exp(-t_jR)$ in each of eqs 1 and 2 by

$$\int_0^{t_{j,max}} \exp(-t_jR)\,dt_j = \frac{1-\exp(-t_{j,max}R)}{R} \tag{4}$$

where $t_{j,max}$ is the maximum value of the t_j time domain. For very large molecules, i.e., in the limit when $\tau \gg 1/R^F_{2,H}$, $t_{j,max} \gg 1/R^F_k$ ($k \in \{2,C; 2,H; MQ\}$), only the last term in each of eqs 1 and 2 becomes important and the ratio of calculated peak intensities in HMQC and HSQC spectra can be approximated by[10]

$$\frac{I_{HMQC}}{I_{HSQC}} \approx \frac{8}{3}\left(\frac{R^S_{2,C}}{R^S_{MQ}}\right) \tag{5}$$

Note that R^S_{MQ} is affected exclusively by relaxation contributions from external spins (neglecting CSA and chemical exchange, eqs 3.4 and 3.6), so in order to achieve optimal sensitivity of methyl correlations in HMQC experiments, it is important to minimize the number of external protons. This is, of course, achieved via extensive deuteration of the protein.[10,11,35]

It follows from the relations given above that for a set of experimental acquisition parameters (τ, $t_{1,max}$, $t_{2,max}$) and for a known value of τ_C, the ratio I_{HMQC}/I_{HSQC} is a function of three variables: (i) S_{axis}^2, (ii) r_{HHext}, and (iii) r_{HDext}. For a methyl-protonated, highly deuterated protein, r_{HDext} does not vary significantly between sites. An average value of 1.80 ± 0.04 Å has been calculated[22] from the coordinates of MSG[30] and is used here. Figure 1 shows contour plots of I_{HMQC}/I_{HSQC} ratios calculated using eqs 1−3 with $t_{1,max} = (3/R^S_{MQ})$ ms and $t_{2,max}$ = 64 ms, which are similar to the values used experimentally, as a function of S_{axis}^2 and r_{HHext} for τ_C = 25 (a) and 150 ns (b). Enhancements larger than ~2.5 ($I_{HMQC}/I_{HSQC} > 2.5$) are predicted for high S_{axis}^2 values *and* for relatively isolated methyl sites, i.e. large r_{HHext} distances. This is a situation rarely realized in practice as it implies an ordered methyl group, likely within the hydrophobic core of a protein, isolated from other methyl protons. I_{HMQC}/I_{HSQC} ratios calculated for S_{axis}^2 = 0.6 (average for the proteins considered here) are plotted as a function of τ_C for several values of r_{HHext} in Figure 2. As expected, I_{HMQC}/I_{HSQC} ratios increase with r_{HHext} and for a given value of r_{HHext} change little for τ_C > ~40 ns. Figure S1 of the Supporting Information plots I_{HMQC}/I_{HSQC} ratios as a function of S_{axis}^2 over a range of r_{HHext}, 2.0 Å ≤ r_{HHext} ≤ 5.0 Å, with τ_C fixed at 100 ns.

dx.doi.org/10.1021/jp401088c | J. Phys. Chem. B 2013, 117, 3571−3577

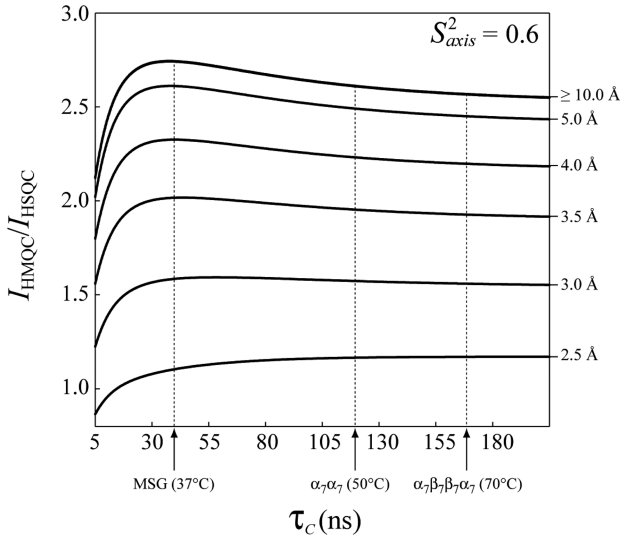

Figure 2. Plots of I_{HMQC}/I_{HSQC} ratios (y-axis) calculated as a function of τ_C (x-axis) for several values of r_{HHext} (Å), with S_{axis}^2 fixed at 0.6. Dashed vertical lines are drawn at approximate τ_C values of MSG at 37 °C, $\alpha_7\alpha_7$ at 50 °C, and $\alpha_7\beta_7\beta_7\alpha_7$ at 70 °C. Calculations have been performed using the same set of parameters as in Figure 1.

Except for very small distances (r_{HHext} < ~2.5 Å), I_{HMQC}/I_{HSQC} ratios are quite sensitive to small changes in S_{axis}^2 and hence are expected to provide a reasonably good measure of side-chain order.

Figure 3 shows the Ile$^{\delta1}$ regions of methyl ^{1}H−^{13}C HMQC correlation maps recorded on samples of [U-^{2}H;Ile$^{\delta1}$-^{13}CH$_3$]-labeled MSG at 37 °C (a), [U-^{2}H;Ile$^{\delta1}$-^{13}CH$_3$;Leu,Val-^{13}CH$_3$/^{12}CD$_3$]-$\alpha_7\alpha_7$ at 50 °C (b), and $\alpha_7\beta_7\beta_7\alpha_7$ proteasome CP, labeled as [U-^{2}H;Ile$^{\delta1}$-^{13}CH$_3$;Leu,Val-^{13}CH$_3$/^{12}CD$_3$] on the two α_7 heptameric rings at 70 °C (c). The corresponding histograms of experimental I_{HMQC}/I_{HSQC} ratios (Figure 3d−f) and R_{MQ}^S rates (Figure 3g−i) for each of the proteins are presented as well. As expected, on the basis of the plots in Figures 1 and 2 showing I_{HMQC}/I_{HSQC} ratios that are essentially invariant of molecular tumbling for correlation times higher than ~40 ns, average values of I_{HMQC}/I_{HSQC} ratios are very similar for the three proteins considered here (Figure 3d−f). Values of $I_{HMQC}/I_{HSQC} \geq 2.7$, obtained when $R_{MQ}^S \leq R_{2,C}^S$ in eq 5, are realized very infrequently and are measured for only two methyl sites among the total of 179 in the three proteins studied (Ile^{592} $\delta1$ in MSG, I_{HMQC}/I_{HSQC} = 2.80 ± 0.03, and Val^{89} $\gamma1$ in $\alpha_7\beta_7\beta_7\alpha_7$, I_{HMQC}/I_{HSQC} = 3.10 ± 0.05). The R_{MQ}^S rates increase approximately linearly with the molecular size of the system, as expected.

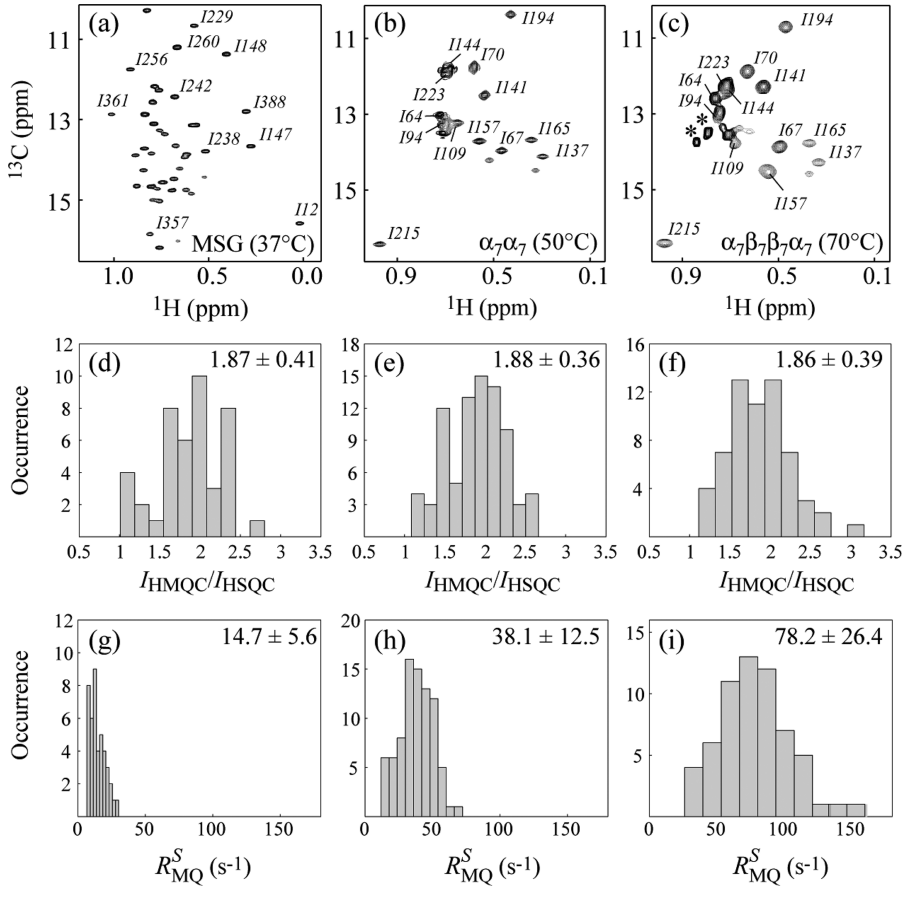

Figure 3. Selected regions of ^{1}H−^{13}C HMQC correlation maps, focusing on Ile$^{\delta1}$ cross-peaks of (a) MSG (37 °C, 600 MHz), (b) $\alpha_7\alpha_7$ (50 °C, 800 MHz), and (c) $\alpha_7\beta_7\beta_7\alpha_7$ (70 °C, 800 MHz), methyl labeled as described in the text. Selected Ile$^{\delta1}$ peak assignments are indicated. The peaks labeled with asterisks in $\alpha_7\beta_7\beta_7\alpha_7$ (c) arise from partial sample degradation. Histograms of experimental I_{HMQC}/I_{HSQC} ratios obtained for each of the protein samples in parts a−c are shown for methyl groups of (d) MSG, (e) $\alpha_7\alpha_7$, and (f) $\alpha_7\beta_7\beta_7\alpha_7$. Histograms of measured R_{MQ}^S rates are shown for (g) MSG, (h) $\alpha_7\alpha_7$, and (i) $\alpha_7\beta_7\beta_7\alpha_7$. The mean and standard deviations are indicated for each distribution.

dx.doi.org/10.1021/jp401088c | J. Phys. Chem. B 2013, 117, 3571−3577

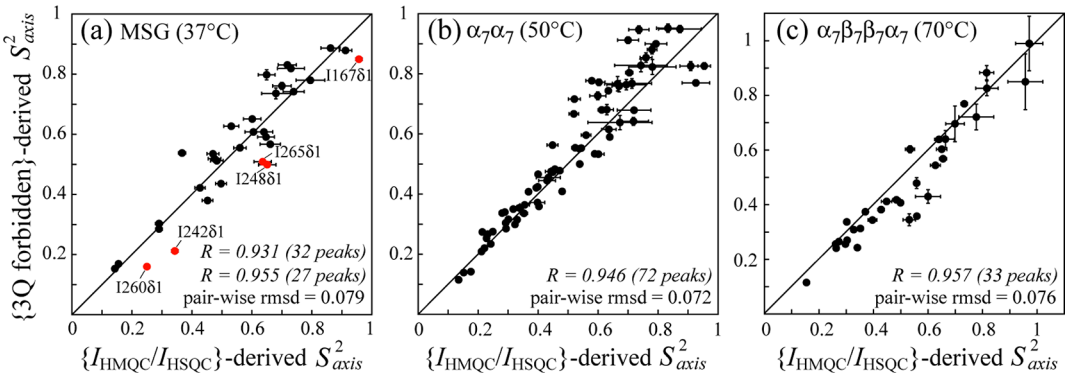

Figure 4. Linear correlation plots of S_{axis}^2 values derived from I_{HMQC}/I_{HSQC} ratios (x-axis) as described in the text versus S_{axis}^2 obtained from $^1H-^1H$ cross-correlated relaxation rates measured using the forbidden 3Q experiment[21] (3Q forbidden, y-axis) for (a) 32 Ile$^{\delta1}$ methyls of MSG (37 °C), (b) 72 methyls of $\alpha_7\alpha_7$ (50 °C), and (c) 33 methyls from the α_7 rings of $\alpha_7\beta_7\beta_7\alpha_7$ (70 °C). For MSG, Pearson correlation coefficients, R, and pairwise rmsd values are shown with and without the inclusion of methyl positions with chemical exchange contributions (red). Linear regression analysis of the correlations in parts a–c yield: (a) $y = (0.01 \pm 0.04) + (0.99 \pm 0.07)x$; (b) $y = (0.01 \pm 0.02) + (1.05 \pm 0.04)x$; (c) $y = (-0.04 \pm 0.03) + (1.00 \pm 0.05)x$.

The dependence of I_{HMQC}/I_{HSQC} on S_{axis}^2 and r_{HHext}, as described above, provides a simple route for obtaining S_{axis}^2 in large perdeuterated proteins, as long as r_{HHext} can be estimated accurately. R_{MQ}^S rates have been measured using the pulse scheme shown in Figure S2 of the Supporting Information. As with HMQC experiments, the inherent sensitivity of R_{MQ}^S measurements is high because only the slowly decaying methyl coherences are of interest. From the obtained values of R_{MQ}^S, site-specific r_{HHext} distances are calculated via eqs 3.6 and 3.7 with r_{HDext} fixed to 1.8 Å. Once r_{HHext} is obtained, S_{axis}^2 can be evaluated via a one-dimensional grid search that minimizes the difference between experimental and calculated (eqs 1–4) I_{HMQC}/I_{HSQC} ratios. This simple two-step procedure does not require estimation of site-specific r_{HHext} distances from protein structures, which is error prone, and can therefore be used for proteins with unknown structures and/or for methyl-containing side chains whose coordinates are missing from the available structural models.

As is clear from inspection of eq 3, the extraction of S_{axis}^2 from I_{HMQC}/I_{HSQC} ratios requires an accurate estimate of τ_C. In the present analysis, we have assumed isotropic molecular tumbling for all protein systems considered. A value of τ_C = 37 ns has been obtained for the relatively low concentrated sample of MSG (250 μM, 100% D_2O, 37 °C) following a procedure described previously.[14,19] For the samples of $\alpha_7\alpha_7$ (50 °C) and $\alpha_7\beta_7\beta_7\alpha_7$ (70 °C), values of 120 and 170 ns, respectively, have been selected so that S_{axis}^2 spans the range between 0 and 1.[17] In order to cross-validate the methodology, we have compared S_{axis}^2 values derived from the I_{HMQC}/I_{HSQC} ratios, as discussed above, with the corresponding values obtained from the 3Q-"forbidden" relaxation-violated coherence transfer scheme that has been described previously.[21] The correlation plots are shown in Figure 4 for Ile$^{\delta1}$ methyls of MSG at 37 °C (a) and for Ile$^{\delta1}$, Leu$^{\delta}$, Val$^{\gamma}$ methyls of $\alpha_7\alpha_7$ at 50 °C (b) and of $\alpha_7\beta_7\beta_7\alpha_7$ at 70 °C (c, α-ring methyls only), with Pearson R values in the range 0.93–0.96 and pairwise rmsd between 0.07 and 0.08, indicating good agreement between the two methods. Of note, these correlations are only slightly inferior to those obtained upon comparison of S_{axis}^2 values derived from different nuclear spin probes in a number of previous studies.[13,16,17,19−21,36] Mean values of the distributions of r_{HHext} calculated from R_{MQ}^S rates for $\alpha_7\alpha_7$ (3.7 ± 0.8 Å) and $\alpha_7\beta_7\beta_7\alpha_7$ (3.3 ± 0.4 Å) are in reasonable agreement with 3.5 ± 1.0 Å calculated from the X-ray structure of the 20S proteasome CP (PDB access code 1pma[31]). The corresponding values for MSG are significantly different (3.7 ± 0.8 Å from R_{MQ}^S vs 5.5 Å from the X-ray structure, PDB access code 1d8c[30]), which reflects minor levels of protonation at additional sites (~3%) in the Ile$^{\delta1}$-labeled sample.

The inherent simplicity of the method does come at a cost, however. Extracted values of S_{axis}^2 are influenced by contributions to line widths (and hence peak intensities) that can arise from chemical exchange. For example, chemical exchange processes that modulate methyl ^1H chemical shifts lower the I_{HMQC}/I_{HSQC} ratio, and to compensate, the extracted values of S_{axis}^2 are reduced accordingly. By contrast, modulation of methyl ^{13}C chemical shifts does not affect the extracted I_{HMQC}/I_{HSQC} ratio since cross-peaks in both HMQC and HSQC data sets are affected equally. Yet, errors in S_{axis}^2 values nevertheless result due to an underestimation of r_{HHext} that in turn elevates the extracted order parameters (eqs 3.4, 3.7, 3.8, 4). Interestingly, the combined effects of chemical exchange contributions to both ^1H and ^{13}C line widths can therefore be partially offset. However, it is often the case that exchange affects only one of the nuclei, leading to more significant errors. We have shown in a previous relaxation dispersion based study of MSG that a number of Ile$^{\delta1}$ methyl sites undergo conformational exchange on the millisecond time scale.[23] Among the residues with the largest discrepancies between the two sets of S_{axis}^2 values in Figure 4a, Ile^{167}, Ile^{242}, Ile^{248}, Ile^{260}, and Ile^{265} all have significant R_{ex} contributions (shown with red), with the largest values corresponding to 21.1, 25.5, and 22.3 s^{-1} for Ile^{242}, Ile^{260}, and Ile^{265}, respectively.[23] Exclusion of these methyl groups from the plot in Figure 4a increases the correlation coefficient to 0.955. A second limitation reflects the fact that to date we have not been able to successfully apply the scheme described above to smaller proteins, although this is not a goal of this work. For example, in an application to [U-^2H;Ile$^{\delta1}$-$^{13}CH_3$;Leu,Val-$^{13}CH_3/^{12}CD_3$]-labeled ubiquitin, 10 °C (τ_C = 9 ns, 100% D_2O), S_{axis}^2 values are overestimated by approximately 0.12, which may result from the assumption of infinitely fast methyl rotation and the simplified model used to extract r_{HHext} values.

As a final note, we remind the reader that we have neglected contributions from ^{13}C and ^1H CSA, both in eq 3 and in calculating order parameters from intensity ratios. Clearly, as

dx.doi.org/10.1021/jp401088c | J. Phys. Chem. B 2013, 117, 3571−3577

the field strength increases, the effects of CSA become more significant. While methyl ^{1}H CSA values are usually very small,[37] contributions from ^{13}C CSA can be larger.[16] For example, assuming an axially symmetric ^{13}C CSA tensor with $\Delta\sigma$ = 25 ppm and S_{axis}^2 = 0.6, CSA relaxation rates are estimated to be 6.4 and 9.0 s^{-1} for $\alpha_7\alpha_7$ and $\alpha_7\beta_7\beta_7\alpha_7$ at 800 MHz, respectively, leading to a decrease in S_{axis}^2 of 0.05 ± 0.02 (0.06 ± 0.03) for $\alpha_7\alpha_7$ ($\alpha_7\beta_7\beta_7\alpha_7$) on average. Because the changes are small, we have chosen not to include CSA effects in the analyses performed here.

CONCLUSIONS

In summary, we have described a simple procedure for approximate evaluation of methyl-containing side-chain mobility in high molecular weight [U-^{2}H;$^{13}CH_3$]-labeled proteins from analysis of simple HSQC and HMQC data sets. The high sensitivity of the spectra, at least in relation to relaxation data sets that are typically recorded for extraction of S_{axis}^2 in such systems, translates into larger numbers of probes that are available for analysis. For example, only 33 of the 95 Ile$^{\delta1}$, Leu, Val methyl sites in the α-subunits of the 670-kDa $\alpha_7\beta_7\beta_7\alpha_7$ complex could be quantified using the 3Q variant of the relaxation-violated coherence transfer experiment, while close to twice the number of residues (61) were analyzed in the HSQC/HMQC scheme described here. The trade-off is that the present approach is only semiquantitative, since extracted order parameter values are sensitive to chemical exchange contributions, which are difficult to estimate without further experiments, and the evaluation of r_{HHext} is necessarily only approximate. Nevertheless, the high sensitivity and the ease-of-use make the method attractive, especially as a first step in analysis of dynamics in supramolecular systems.

ASSOCIATED CONTENT

Supporting Information

Figure S1 showing plots of I_{HMQC}/I_{HSQC} ratios calculated as a function of S_{axis}^2 for several values of r_{HHext}, with τ_C fixed at 100 ns and Figure S2 showing the pulse scheme for the measurement of R_{MQ}^S rates. This material is available free of charge via the Internet at http://pubs.acs.org.

AUTHOR INFORMATION

Corresponding Author

*E-mail: vitali@umd.edu. Tel: +1-301-4051504. Fax: +1-301-3140386.

Notes

The authors declare no competing financial interest.

ACKNOWLEDGMENTS

The authors thank Drs. Daoning Zhang and Chenyun Guo (University of Maryland) for preparation of samples of ubiquitin and MSG, and Drs. Amy Ruschak (Case Western University) and Remco Sprangers (Max Planck Institute for Developmental Biology, Tübingen, Germany) for preparation of samples of $\alpha_7\alpha_7$ and $\alpha_7\beta_7\beta_7\alpha_7$ when they were in the Kay laboratory. This work was supported by grants from the Canadian Institutes of Health Research and the Natural Sciences and Engineering Research Council of Canada. L.E.K. holds a Canada Research Chair in Biochemistry.

REFERENCES

(1) Metzler, W. J.; Wittekind, M.; Goldfarb, V.; Mueller, L.; Farmer, B. T. Incorporation of $^{1}H/^{13}C/^{15}N$-{Ile,Leu,Val} into a Perdeuterated, ^{15}N-Labeled Protein: Potential in Structure Determination of Large Proteins by NMR. *J. Am. Chem. Soc.* **1996**, *118*, 6800−1.

(2) Gardner, K. H.; Rosen, M. K.; Kay, L. E. Global Folds of Highly Deuterated, Methyl Protonated Proteins by Multidimensional NMR. *Biochemistry* **1997**, *36*, 1389−401.

(3) Goto, N. K.; Kay, L. E. New Developments in Isotope Labeling Strategies for Protein Solution NMR Spectroscopy. *Curr. Opin. Struct. Biol.* **2000**, *10*, 585−92.

(4) Tugarinov, V.; Kanelis, V.; Kay, L. E. Isotope Labeling Strategies for the Study of High-Molecular-Weight Proteins by Solution NMR Spectroscopy. *Nat. Protoc.* **2006**, *1*, 749−54.

(5) Sprangers, R.; Velyvis, A.; Kay, L. E. Solution NMR of Supramolecular Complexes: Providing New Insights into Function. *Nat. Methods* **2007**, *4*, 697−703.

(6) Ruschak, A. M.; Kay, L. E. Methyl Groups as Probes of Supra-Molecular Structure, Dynamics and Function. *J. Biomol. NMR* **2010**, *46*, 75−87.

(7) Tang, Y.; Schneider, W. M.; Shen, Y.; Raman, S.; Inouye, M.; Baker, D.; Roth, M. J.; Montelione, G. T. Fully Automated High-Quality NMR Structure Determination of Small ^{2}H-Enriched Proteins. *J. Struct. Funct. Genomics* **2010**, *11*, 223−32.

(8) Sheppard, D.; Sprangers, R.; Tugarinov, V. Experimental Approaches for NMR Studies of Sidechain Dynamics in High-Molecular-Weight Proteins. *Prog. Nucl. Magn. Reson. Spectrosc.* **2010**, *56*, 1−45.

(9) Kay, L. E. Solution NMR Spectroscopy of Supra-Molecular Systems, Why Bother? A Methyl-Trosy View. *J. Magn. Reson.* **2011**, *210*, 159−70.

(10) Tugarinov, V.; Hwang, P. M.; Ollerenshaw, J. E.; Kay, L. E. Cross-Correlated Relaxation Enhanced $^{1}H-^{13}C$ NMR Spectroscopy of Methyl Groups in Very High Molecular Weight Proteins and Protein Complexes. *J. Am. Chem. Soc.* **2003**, *125*, 10420−8.

(11) Tugarinov, V.; Hwang, P. M.; Kay, L. E. Nuclear Magnetic Resonance Spectroscopy of High-Molecular-Weight Proteins. *Annu. Rev. Biochem.* **2004**, *73*, 107−46.

(12) Ishima, R.; Louis, J. M.; Torchia, D. A. Transverse C-13 Relaxation of CHD_2 Methyl Isotopomers To Detect Slow Conformational Changes of Protein Side Chains. *J. Am. Chem. Soc.* **1999**, *121*, 11589−90.

(13) Ishima, R.; Petkova, A. P.; Louis, J. M.; Torchia, D. A. Comparison of Methyl Rotation Axis Order Parameters Derived from Model-Free Analyses of ^{2}H and ^{13}C Longitudinal and Transverse Relaxation Rates Measured in the Same Protein Sample. *J. Am. Chem. Soc.* **2001**, *123*, 6164−71.

(14) Tugarinov, V.; Ollerenshaw, J. E.; Kay, L. E. Probing Side-Chain Dynamics in High Molecular Weight Proteins by Deuterium NMR Spin Relaxation: An Application to an 82-kDa Enzyme. *J. Am. Chem. Soc.* **2005**, *127*, 8214−25.

(15) Tugarinov, V.; Kay, L. E. A ^{2}H NMR Relaxation Experiment for the Measurement of the Time Scale of Methyl Side-Chain Dynamics in Large Proteins. *J. Am. Chem. Soc.* **2006**, *128*, 12484−9.

(16) Tugarinov, V.; Kay, L. E. Quantitative ^{13}C and ^{2}H NMR Relaxation Studies of the 723-Residue Enzyme Malate Synthase G Reveal a Dynamic Binding Interface. *Biochemistry* **2005**, *44*, 15970−7.

(17) Sprangers, R.; Kay, L. E. Quantitative Dynamics and Binding Studies of the 20S Proteasome by NMR. *Nature* **2007**, *445*, 618−22.

(18) Godoy-Ruiz, R.; Guo, C.; Tugarinov, V. Alanine Methyl Groups as NMR Probes of Molecular Structure and Dynamics in High-Molecular-Weight Proteins. *J. Am. Chem. Soc.* **2010**, *132*, 18340−50.

(19) Tugarinov, V.; Kay, L. E. Relaxation Rates of Degenerate ^{1}H Transitions in Methyl Groups of Proteins as Reporters of Side-Chain Dynamics. *J. Am. Chem. Soc.* **2006**, *128*, 7299−308.

(20) Tugarinov, V.; Sprangers, R.; Kay, L. E. Probing Side-Chain Dynamics in the Proteasome by Relaxation Violated Coherence Transfer NMR Spectroscopy. *J. Am. Chem. Soc.* **2007**, *129*, 1743−50.

(21) Sun, H.; Kay, L. E.; Tugarinov, V. An Optimized Relaxation-Based Coherence Transfer NMR Experiment for the Measurement of Side-Chain Order in Methyl-Protonated, Highly Deuterated Proteins. *J. Phys. Chem. B* **2011**, *115*, 14878−84.
(22) Ollerenshaw, J. E.; Tugarinov, V.; Kay, L. E. Methyl Trosy: Explanation and Experimental Verification. *Magn. Reson. Chem.* **2003**, *41*, 843−52.
(23) Korzhnev, D. M.; Kloiber, K.; Kanelis, V.; Tugarinov, V.; Kay, L. E. Probing Slow Dynamics in High Molecular Weight Proteins by Methyl-Trosy NMR Spectroscopy: Application to a 723-Residue Enzyme. *J. Am. Chem. Soc.* **2004**, *126*, 3964−73.
(24) Bax, A.; Griffey, R. H.; Hawkings, B. L. Correlation of Proton and Nitrogen-15 Chemical Shifts by Multiple Quantum NMR. *J. Magn. Reson.* **1983**, *55*, 301−15.
(25) Mueller, L. Sensitivity Enhanced Detection of Weak Nuclei Using Heteronuclear Multiple Quantum Coherence. *J. Am. Chem. Soc.* **1979**, *101*, 4481−4.
(26) Bodenhausen, G.; Ruben, J. Natural Abundance Nitrogen-15 NMR by Enhanced Heteronuclear Spectroscopy. *Chem. Phys. Lett.* **1980**, *69*, 185−9.
(27) Pervushin, K.; Riek, R.; Wider, G.; Wüthrich, K. Attenuated T_2 Relaxation by Mutual Cancellation of Dipole−Dipole Coupling and Chemical Shift Anisotropy Indicates an Avenue to NMR Structures of Very Large Biological Macromolecules in Solution. *Proc. Natl. Acad. Sci. U.S.A.* **1997**, *94*, 12366−71.
(28) Pervushin, K.; Riek, R.; Wider, G.; Wüthrich, K. Transverse Relaxation-Optimized Spectroscopy (Trosy) for NMR Studies of Aromatic Spin Systems in ^{13}C-labeled Proteins. *J. Am. Chem. Soc.* **1998**, *120*, 6394−400.
(29) Miclet, E.; Williams, D. C., Jr; Clore, G. M.; Bryce, D. L.; Boisbouvier, J.; Bax, A. Relaxation-Optimized NMR Spectroscopy of Methylene Groups in Proteins and Nucleic Acids. *J. Am. Chem. Soc.* **2004**, *126*, 10560−70.
(30) Howard, B. R.; Endrizzi, J. A.; Remington, S. J. Crystal Structure of *Escherichia coli* Malate Synthase G Complexed with Magnesium and Glyoxylate at 2.0 Å Resolution: Mechanistic Implications. *Biochemistry* **2000**, *39*, 3156−68.
(31) Löwe, J.; Stock, D.; Jap, B.; Zwickl, P.; Baumeister, W.; Huber, R. Crystal Structure of the 20S Proteasome from the Archaeon *T. Acidophilum* at 3.4 Å Resolution. *Science* **1995**, *268*, 533−9.
(32) Guo, C.; Zhang, D.; Tugarinov, V. An NMR Experiment for Simultaneous Trosy-Based Detection of Amide and Methyl Groups in Large Proteins. *J. Am. Chem. Soc.* **2008**, *130*, 10872−73.
(33) Delaglio, F.; Grzesiek, S.; Vuister, G. W.; Zhu, G.; Pfeifer, J.; Bax, A. NMRpipe: A Multidimensional Spectral Processing System Based on Unix Pipes. *J. Biomol. NMR* **1995**, *6*, 277−93.
(34) Kamith, U.; Shriver, J. W. Characterization of the Thermotropic State Changes in Myosin Subfragment-1 and Heavy Meromyosin by UV Difference Spectroscopy. *J. Biol. Chem.* **1989**, *264*, 5586−92.
(35) Tugarinov, V.; Kay, L. E. Methyl Groups as Probes of Structure and Dynamics in NMR Studies of High-Molecular-Weight Proteins. *ChemBioChem* **2005**, *6*, 1567−77.
(36) Sun, H.; Godoy-Ruiz, R.; Tugarinov, V. Estimating Side-Chain Order in Methyl-Protonated, Perdeuterated Proteins Via Multiple-Quantum Relaxation Violated Coherence Transfer NMR Spectroscopy. *J. Biomol. NMR* **2012**, *52*, 233−43.
(37) Tugarinov, V.; Scheurer, C.; Brüschweiler, R.; Kay, L. E. Estimates of Methyl ^{13}C and ^{1}H CSA Values ($\Delta\sigma$) in Proteins from Cross-Correlated Spin Relaxation. *J. Biomol. NMR* **2004**, *30*, 397−406.